

WIRE-LINE LOGGING ANALYSIS OF THE 2007 JOGMEC/NRCAN/AURORA MALLIK GAS HYDRATE PRODUCTION TEST WELL

Tetsuya Fujii*, Tokujiro Takayama, Masaru Nakamizu, Koji Yamamoto**
Technology & Research Center, Japan Oil, Gas and Metals National Corporation
1-2-2 Hamada, Mihama-ku, Chiba, 261-0025, JAPAN

Scott Dallimore, Jonathan Mwenifumbo, Fred Wright
Geological Survey of Canada, Natural Resources Canada
9860 West Saanich Road, Sidney, BC V8L 4B2, CANADA

Masanori Kurihara, Akihiko Sato
Japan Oil Engineering Company
1-7-3 Kachidoki, Chuo-ku, Tokyo, 104-0054, JAPAN

Ahmed Al-Jubori
Schlumberger Canada Ltd.
525 3rd Ave SW, Calgary, AB, CANADA

ABSTRACT

In order to evaluate the productivity of methane hydrate (MH) by the depressurization method, Japan Oil, Gas and Metals National Corporation and Natural Resources Canada carried out a full scale production test in the Mallik field, Mackenzie Delta, Canada in April, 2007. An extensive wire-line logging program was conducted to evaluate reservoir properties, to determine production/water injection intervals, to evaluate cement bonding, and to interpret MH dissociation behavior throughout the production. New open hole wire-line logging tools such as MR Scanner, Rt Scanner and Sonic Scanner, and other advanced logging tools such as ECS (Elemental Capture Spectroscopy) were deployed to obtain precise data on the occurrence of MH, lithology, MH pore saturation, porosity and permeability. Perforation intervals of the production and water injection zones were selected using a multidisciplinary approach. Based on the results of geological interpretation and open hole logging analysis, we picked candidate test intervals considering lithology, MH pore saturation, initial effective permeability and absolute permeability. Reservoir layer models were constructed to allow for quick reservoir numerical simulations for several perforation scenarios. Using the results of well log analysis, reservoir numerical simulation, and consideration of operational constraints, a MH bearing formation from 1093 to 1105 mKB was selected for 2007 testing and three zones (1224-1230, 1238-1256, 1270-1274 mKB) were selected for injection of produced water.

Three kinds of cased-hole logging, RST (Reservoir Saturation Tool), APS (Accelerator Porosity Sonde), and Sonic Scanner were carried out to evaluate physical property changes of MH bearing formation before/after the production test. Preliminary evaluation of RST-sigma suggested that MH bearing formation in the above perforation interval was almost selectively dissociated (sand produced) in lateral direction. Preliminary analysis using Sonic Scanner data, which has deeper depth of investigation than RST brought us additional information on MH dissociation front and dissociation behavior.

* Corresponding author: Phone: +81 43 276 9243 Fax +81 43 276 4062 E-mail: fujii-tetsuya@jogmec.go.jp

** Present address: Research Center, Japan Petroleum Exploration Co., Ltd., 1-2-1 Hamada, Mihama-ku, Chiba, 261-0025, JAPAN

Ca, Fe, S, Ti, Gd, K) [10]. In this project, it was mainly used for the absolute permeability evaluation.

Sonic Scanner measures compressional, shear and stoneley waves. The tool is used to evaluate formation elastic/mechanical properties at multiple depths of investigation and acoustic anisotropy. The source of the acoustic anisotropy can be discriminated as to whether it is intrinsic or stress-induced [10]. These advanced sonic measurements enabled an increased understanding of both the MH characteristics and formation geomechanics.

Rt Scanner is a triaxial induction tool that calculates vertical and horizontal resistivities (Rv,

Rh) from direct measurements, while simultaneously solving for formation dip at any well deviation including anisotropic formations [10]. Its multiple depths of investigation in all three dimensions ensures that derived resistivities are a true 3D measurement.

MR Scanner is the latest generation of magnetic resonance tools. It has the capability of recording multiple depths of investigation in a single pass. Its measurement sequence allows a profiled view of the reservoir fluids. Deeper and multiple depths of investigation make it easier to detect any data-quality problems associated with rugose boreholes, mudcake, and fluids in various hole sizes [10].

Table 1. Open hole wire-line logging program in Mallik 2L-38 (2007).

Run	Date	Depth interval	Logging tool
pre-logging	March 3, 2007	850-1121	AIT-TLD-HGNS-CMR-EMS
#1	March 6, 2007	680-1276	GR-PPC-GPIT-EMS-HRLT-SP-Rt Scanner
#2	March 6 and 7, 2007	680-1268	GR-PPC-HNGS-ECS-CMR-HGNS-HRMS-APS
#3	March 9, 2007	680-1279	GR-PPC-Sonic Scanner-FMI
#4	March 9, 2007	1296-1308	GR-HGNS-TLD-AIT-SP
#5	March 9 and 10, 2007	850-1150	GR-MR Scanner-HGNS

Formal nomenclatures and applications

AIT Array Induction Image Tool) : Induction resistivity, SP, Rm
 APS Accelerator Porosity Sonde) : Neutron porosity index, Formation sigma
 CMR Combinable Magnetic Resonance Tool) : Total NMR porosity, NMR free-fluid porosity, Permeability
 ECS Elemental Capture Spectroscopy Sonde) : Lithology fractions, Formation elements (Si, Fe, Ca, S, Ti, Gd, Cl, Ba, H)
 EMS Environmental Measurement Sonde) : Mud resistivity, Mud temperature, Caliper
 FMI Fullbore Formation MicroImager) : High-resolution electrical images
 GR Gamma Ray) : Gamma ray
 GPIT General Purpose Inclination Tool) : Borehole azimuth, deviation, Tool azimuth
 HGNS Highly Integrated Gamma Ray Neutron Sonde) : Gamma ray, Neutron porosity
 HNGS Hostile Natural Gamma Ray Sonde) : Gamma ray
 HRLT High Resolution Laterolog Array Tool) : High resolution resistivity
 HRMS High-Resolution Mechanical Sonde) : Bulk density, PEF, Caliper, Microresistivity
 MR Scanner Magnetic Resonance Scanner) : Total NMR porosity, NMR free-fluid porosity, Permeability
 PPC Power Positioning Caliper Tool) : Caliper
 Rt Scanner Triaxial Induction Scanner) : Rv, Rh, AIT logs, SP, Dip, Azimuth
 Sonic Scanner Acoustic Scanning Platformforms) : DTp, DTs, Full waveforms, Cement bond quality waveforms
 SP Spontaneous Potential) : Spontaneous potential
 TLD Three-Detector Lithology Density) : Lithology density

Perforation intervals selection workflow

The 2007 Mallik 2L-38 production well was advanced to 1310m (RKB) to allow for downhole gas/water separation and re-injection of produced water in the same well. Perforation intervals for the water injection and production zones were selected using a multidisciplinary approach by considering the reservoir properties of MH bearing zones interpreted from well log analysis, productivity and water injectivity predicted from quick reservoir numerical simulation, cement bonding conditions, and operational constraints. Figure 2 shows the work flow applied in the determination of the perforation intervals in 2L-38 (2007).

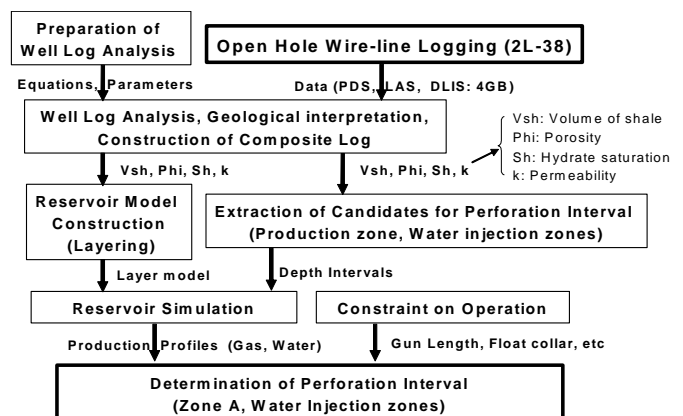


Figure 2. Work flow for the determination of perforation intervals in 2L-38 (2007).

Well log analysis in the production zone

(a) Well log analysis method

Figure 3 shows an example of composite chart of 2L-38 (2007) derived from the open hole wire-line logging data in one of the MH bearing zones (zone A). Technical details of these open hole well log analysis are also described in [2].

For the basis of reservoir model construction, volume of shale (Vsh), effective porosity (PhiE), hydrate pore saturation (Sh), initial effective permeability (Kint), and absolute permeability (Ka) were analyzed using the logging data.

Vsh was evaluated using natural gamma ray log (GR, T2 column in Figure 3) through following equation with GR response in clean sand (GRclean) and shale interval (GRshale).

$$Vsh = (GR - GR_{clean}) / (GR_{shale} - GR_{clean}) \quad (1)$$

PhiE was evaluated based on density porosity (PhiD, T4 column in Figure 3), together with Vsh correction using following equations.

$$PhiE = PhiD (1 - Vsh) \quad (2)$$

$$PhiD = (\rho_{ma} - \rho_b) / (\rho_{ma} - \rho_f) \quad (3)$$

ρ_{ma} : matrix density (2.65 g/cm³ was used)

ρ_b : bulk density (g/cm³)

ρ_f : fluid density (1.0 g/cm³ was used)

Sh was estimated using the combination of total CMR porosity (TCMR, T4 column in Figure 3) and PhiD through DMR (Density-Magnetic-Resonance) method [11, 12] using following equation.

$$Sh = (PhiD - TCMR) / PhiD \quad (4)$$

Estimation results were shown in T6 column in Figure 3.

Kint was estimated by analyzing CMR log using both SDR (Schlumberger-Doll Research) method (KSDR, [13]) and Timur-Coates method (KTIM, [14]), with following equations and parameters.

$$KSDR (md) = C * TCMR^4 * T2LM^2 \quad (5)$$

C: mineralogy constant (4000 D/s² = 4 md/s² [15])

T2LM: T2 logarithmic mean (milli-seconds)

$$KTIM (md) = a * TCMR^4 * (FFV/BFV)^2 \quad (6)$$

a: constant (10,000 was used)

TCMR: Total NMR porosity

FFV: NMR Free Fluid Volume

BFV: NMR bound Fluid Volume

Generally, KTIM shows higher value than KSDR using above constants (T7 column in Figure 3). We used KSDR for initial effective permeability input as base case, mainly because the number of uncertain parameter is smaller than KTIM.

Ka was evaluated using both empirical model constructed by JOE (Ka_JOE) [6] and model derived from ECS (Ka_ECS) [16]. Ka_JOE is based on the well log calibration results using actual core samples from Mallik 5L-38 and it is the function of PhiE, Vsh, and Sh [6]. On the other hand, Ka_ECS is mainly governed by weight fraction of clay, which is based on core database of mineralogy and chemistry measured on 400 samples [16]. Both permeability evaluations were shown in T7 column in Figure 3. These two models show discrepancy in shaley intervals, which is attributed to the difference in correction method for shale volume. We used Ka_JOE for the base case because it is based on actual Mallik core samples, while Ka_ECS was used for sensitivity analysis.

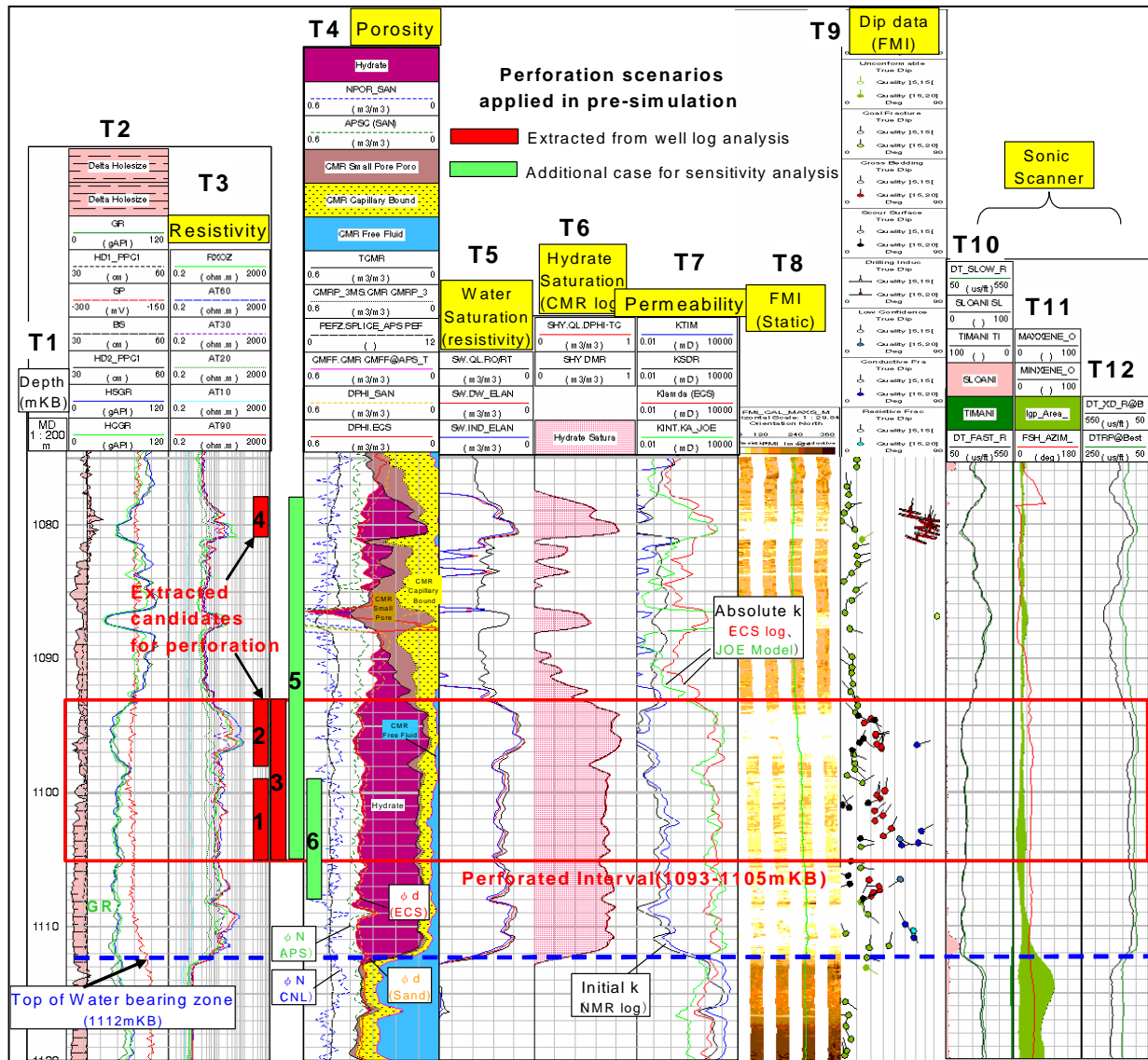
(b) Criteria for selection of perforation interval for production well

We have picked up candidates for the perforation interval based on the results of geological interpretation, well log analysis mentioned above, and the following criteria (Table 2) suggested by Japan Oil Engineering Company (JOE)/AIST, based on the past reservoir simulations.

- (a) Sandy formations: identified mainly from the gamma-ray log curve.
- (b) High initial effective permeability (rough measure is higher than 0.5 md): evaluated from CMR log (Figure 3, column T7).
- (c) Moderate degree of MH pore saturation (rough measure is around 60 %): Evaluated from CMR and density logs (Figure 3, column T6). 60 % is a preferable MH saturation figure in terms of dissociation efficiency, because if the MH saturation is too high, then the initial effective permeability becomes too low.
- (d) Enough vertical distance from the top of the water bearing zone (rough measure is more than 5 m): Evaluated from resistivity and CMR logs. The top of the water bearing zone was interpreted to be around 1,112 mKB (Figure 3). The objective was to avoid water production (coning) by depressurization.
- (e) Existence of a seal formation between water bearing zones.

By considering the above criteria and other geological features such as fracture distribution (FMI, Figure 3, column T8 and T9), coal layers

(Sonic, Density, ECS), we extracted four possible candidates for the production zone as shown in Figure 3 (Red bar).



Track No.	Parameters	Units	Comments
T1	Depth	mKB	KB=11.8mMSL
T2	GR, SP, Caliper, etc	API, mV, cm, etc	
T3	Resistivity (HRLT)	ohm.m	
T4	Porosity (ϕ_d sand, TCMR, ϕ_{Pef} , ϕ_d ECS, etc)	fraction	ϕ_d ECS is slightly larger than ϕ_d sand [2]
T5	Sw (Ro/Rt, Indonesian Eq, DW model)	fraction	Indo and DW are almost the same
T6	Sh from CMR (quick look (overlay) and DMR)	fraction	Both models have similar output
T7	Permeability (KSDR, KTIM, Ka_ECS, Ka_JOE)	fraction	Technical details are also described in [2]
T8	FMI (Static image)	degree	
T9	Dip data from FMI	degree	Fracture dips were classified by confidence level.
T10	DT-slow, DT-fast, slow-fast	us/ft	Difference of slowness between fast and slow [2].
T11	X-line energy (max, min) Fast azimuth		Anisotropy
T12	Delta-T	us/ft	Hydrate saturation [2].

Figure 3. An example of the composite chart of 2L-38 (2007) open hole logging data in a MH bearing zone (zone A) and extracted perforation candidates.

Table 2. Criteria for determining the production zone (zone A) and the tools used for evaluation.

	Measurement Items	Criteria	Tools for decision	Log analysis method
(a)	Lithology of sediments	Sandy layer	GR, HNGS, ECS, (Cuttings)	
(b)	Initial effective permeability	> 0.5md	CMR, MR Scanner	SDR (Kenyon, 1992) (KSDR) [13] Timur&Coates (KTIM) [14]
(c)	MH pore saturation	Around 60%	CMR, Resistivity	DMR method [11, 12]
(d)	Vertical distance from water bearing zone	> 5m	Resistivity, CMR	
(e)	Existence of seal formation between water bearing formation		GR, HNGS, ECS	

Quick reservoir simulation

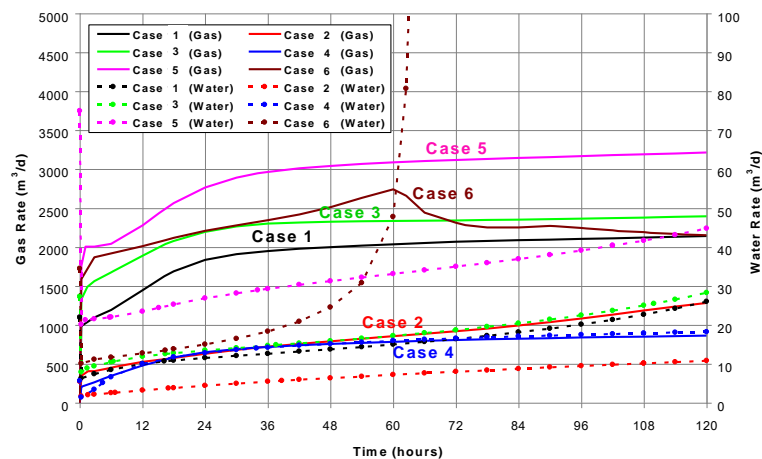
Based on four candidate intervals for perforation (Figure 3) and reservoir layered model constructed reflecting the above well log analysis, JOE/AIST carried out a quick reservoir numerical simulation for the determination of perforation interval (pre-simulation). For this reservoir simulation, MH21-HYDRES (MH21 Hydrate Reservoir Simulator) [17, 18] was used. This simulator is able to deal with three-dimensional, five-phase, four-component problems [17, 18].

Reservoir layer model was constructed for the simulation input based on the well log analysis results already mentioned above. Detail parameters and settings of the model are described in [6].

Besides four perforation candidates extracted from the well log analysis, two additional scenarios were assumed for sensitivity analysis. Therefore, the simulation was conducted assuming totally six perforation scenarios (Figure 3, 4).

Case	Perforation interval (mKB)
Case 1	1099 - 1105
Case 2	1093 - 1098
Case 3	1093 - 1105
Case 4	1078 - 1081
Case 5	1078 - 1098
Case 6	1099 - 1108

Figure 4. Prediction of production test performance by JOE for the determination of perforation interval.



Free gas indication

While not conclusive, examination of the V_p/V_s ratio from 1998 sonic log in Mallik 2L-28 well suggested a thin free-gas-bearing interval just below the lower most hydrate bearing zone [8]. In order to investigate the possibility of existence of free gas layer, we checked open hole logging data.

Free gas layers are usually identified by the separation between density porosity (DPHI) and

Figure 4 shows an example of simulated production performances for 5 days. The solid lines show the predicted gas production rates, while the dashed lines show the predicted water production rates. 3 MPa was assumed as a bottom hole pressure in all the cases. Gas production of 1,000-3,000 m³/d and water production of 10-40 m³/d were predicted. It was anticipated that if the perforation interval is shorter like Cases 2 (5 m) and 4 (3 m), the production rates should be lower. It was also simulated that if there wasn't an enough vertical distance from the top of water bearing zone as shown in case 6 (4 m), water coning could happen at an early stage (in this case, within 2.5 days).

Considering the conditions of (1) higher gas production rate and (2) lower water production rate, it was concluded that Case 3 is the most preferable.

neutron porosity (NPOR) curves in well log data (DPHI>NPOR, Figure 3). We also utilized density porosity derived from the ECS log (DPHI.ECS) and 2 kinds of neutron porosity derived from the APS log for more precise analysis (APSC in Figure 3 is neutron porosity with shallower depth of investigation). As a result of overlaying these density and neutron porosity logs, we did not see

any significant gas indication within the surveyed interval (820 to 1270 mMSL) (Figure 3).

We also compared Vp/Vs obtained from Sonic Scanner this time with Vp/Vs obtained from sonic log in 1998, as shown in Figure 5. We could not find significantly low Vp/Vs interval around the top of water bearing zone like 2L-38 (1998), which suggests no significant gas bearing layer.

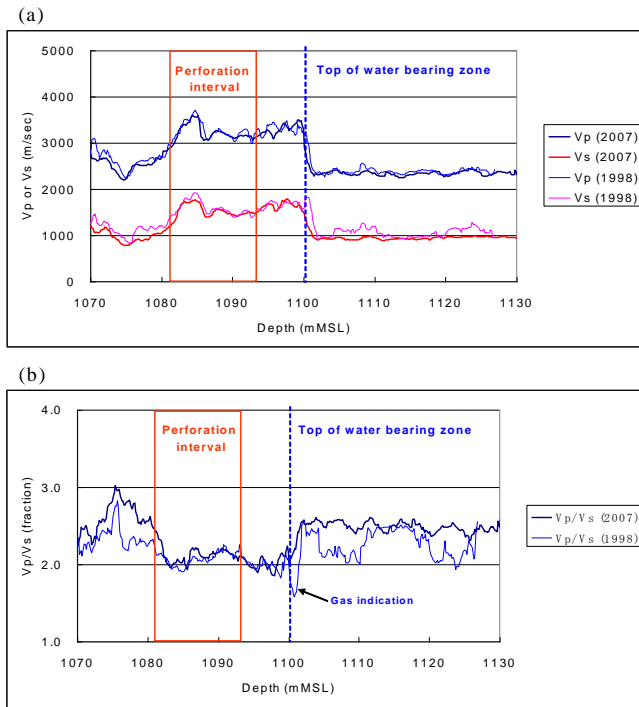


Figure 5. Comparison of Vp, Vs, and Vp/Vs between obtained in 2007 and 1998, respectively. (a) comparison of Vp and Vs. (b) comparison of Vp/Vs. Considering the KB hight (11.8mMSL), perforated interval 1093-1105 mKB (2007) is 1081-1093 mMSL, while the top of water bearing zone 1112 mKB (2007) is 1100 mMSL.

Determination of perforation intervals

Considering the reservoir properties of MH bearing zones derived from well log analysis, gas productivity and water injectivity predicted from reservoir numerical simulation, cement bonding condition, and operational constraints such as perforation gun lengths (6m base) and time constraints, we selected the following perforation intervals.

- (a) Production test zone (A zone)
1093-1105 mKB (12m continuous, Case 3 in Figure 4)
- (b) Produced water injection zone
1224-1230, 1238-1256, 1270-1274 mKB

CASED HOLE LOGGING

There were two main objectives for undertaking cased hole logging in Mallik 2L-38 (2007). The first objective was cement evaluation, which is important for the optimization of well completion such cement volume estimation, and confirmation of monitoring cable location. The second objective was to evaluate physical property changes (MH dissociation behavior) of hydrate bearing formations throughout the production test.

In this paper, we will focus on the second objectives and related study results.

Measurement items

For the cement bond evaluation in 2L-38 (2007), we used new logging tools such as the Isolation Scanner*, in addition to conventional evaluation tools such as CBL-VDL (Sonic Scanner). Both tools were used simultaneously to confirm the exact location and distribution of the monitoring cables for safe perforation.

In the Mallik 2002 project, CHFR* (Cased Hole Formation Resistivity) was used for the evaluation of MH dissociation [9]. However we could not use the CHFR in this project due to the presence of a plastic coating (yellow jacket) behind the casing, which was installed for electrical resistivity monitoring purpose [4]. For that reason, we used RST (Reservoir Saturation Tool), APS (Accelerator Porosity Sonde), and Sonic Scanner for MH dissociation evaluation instead. Table 3 shows the cased hole wire-line logging program conducted in Mallik 2L-38 (2007).

Table3. Cased hole wire-line logging program in Mallik 2L-38 (2007).

	Run	Date	Logging tool	Mode	Depth (mKB)
Before Test	1	March 23, 2007	Sonic Scanner-Isolation Scanner-GR-CCL	CBL-VDL Concise USI IBC	30-1273 850-1273 850-1273 30-1273
	2	March 23-24, 2007	APS-GR-CCL		850-1273
	3	March 24, 2007	RST(Sigma, C/O)-GR-CCL		820-1270
After Test	1	April 7-8, 2007	Sonic Scanner -APS-GR-CCL	CBL-VDL RAD BARS APS	850-1195 850-1193 850-1193 850-1208
	2	April 8-9, 2007	RST(Sigma)-GR-CCL	Sigma only	850-1206
	3	April 9, 2007	Isolation Scanner-GR-CCL	IBC, USI	1040-1209

GR Gamma Ray
CCL Casing Collar Locator

RST is a saturation evaluation tool that uses a minitron instead of a chemical neutron source. It utilizes two kinds of reactions between atoms in

the formation and fast neutrons, i.e. neutron capture and inelastic scattering. RST sigma is the measurement of the gamma-ray count (capture gamma-ray) emitted from atoms excited by the neutron capture reaction, which can give us information about fluid saturation [19]. Pure water and carbon (oil, MH) have similar neutron capture sections, while chlorine is more reactive with neutron and has a larger cross section. Therefore, RST sigma can be an indicator of salinity change in formation water.

An outline of APS and Sonic Scanner has already been described in previous sections of this paper.

These cased hole logging measurements were utilized for the analysis of physical property changes throughout the production test.

RST results

Figure 6 shows some differences in the RST and APS log responses between before and after the production test. Depth of investigation of RST is 10 in (25.4 cm) [10], and the detector faces the inner surface of casing during logging. Taking into consideration the difference between the inner diameter of casing and the borehole diameter, the actual depth of investigation of RST is about 19 cm from open hole wall (Figure 7).

Black dashed lines and red solid lines in Figure 6 show the depth plot of parameters before and after the production test, respectively. The area within the red box is the production (perforated) interval. Throughout the production test, some changes in the log response were noticed, such as a significant selective decrease in inelastic scattering signal (T1), a selective increase in thermal decay signal (T4), and a selective increase in RST sigma (T5), in the perforated interval. A small change in the same parameters just 1m above and 3m below the perforated interval was noticed too, but to a lesser degree.

We also recognized that above parameters in high MH saturation intervals just below the perforated interval (1108-1112 mKB) did not change throughout the production. These results suggest that MH bearing formations at the perforated interval was almost selectively dissociated / sand produced in a lateral direction. That suggests the possibility of water invasion from water bearing zones behind casing (water coning) is small, because formation water inversion would have caused MH dissociation, and these parameters would have changed as a result.

APS results

Figure 6 (right) shows the difference in APS outputs before and after the production test. Actual depth of investigation from the open hole wall is about 11cm when considering the casing diameter (Figure 7). Generally speaking, repeatability of the ASP curves was much poorer than the RST, and that was the case when overlaying two passes of the same descent in hole. The major factor causing that is the relatively small depth of investigation compared to the open hole size.

In spite of these difficulties, we were able to recognize a selective increase in neutron porosity (APSC, T6) between before and after the production test in the perforated interval.

Sonic Scanner results

After the processing and re-picking we recognized the following velocity changes in P-wave (Compressional) and S-wave (Shear) from the Sonic Scanner, which has a deeper depth of investigation than APS and RST (P-wave: 20-40 cm from borehole wall, S-wave: 30-60 cm from borehole wall, in this case, Figure 7), in the perforated interval [20].

- (1) P-wave, which was detected before the production test, could not be detected in the lower part of the perforated interval after the test (indicating gas existence) (Figure 7, right).
- (2) S-wave velocity at the lower part of the perforated interval decreased to the velocity level of a water bearing zone (Figure 7, right). This velocity decreased happened in the zone of with higher initial effective permeability suggested from the CMR log (middle of Figure 7).

DISCUSSION

As discussed in the previous section, the following changes in RST and APS response were recognized in perforated interval (1093-1105 mKB), in spite of the relatively shallower depth of investigation (about 19cm and 11cm from open hole wall, respectively) (Figure 6 and 8).

- (1) Selective increase in RST sigma and APS, which corresponds to the number of chlorine atoms and hydrogen atoms, respectively.
- (2) Selective decrease in the inelastic scattering, which corresponds to the number of carbon atoms.

The increase in RST sigma can be a reflection of an increase in formation salinity (chloride atoms

number), i.e. replacement of MH bearing formation behind casing by well bore fluid (Brine@KCl 5 %) or formation water. There are three possible replacement scenarios; (1) into the sand pore space, (2) cavity space, or (3) a combination of both. However, from the RST data alone we can not distinguish these scenarios. We also need to consider about not only fluid movement, but also sediment movement (grain rearrangements) induced by sanding. Clearly there are a number of complex considerations to be evaluated.

Based on the observations and analysis above, following interpretation on MH dissociation process could be possible as one hypothesis (Figure 9).

- (1) MH bearing sands are composed of a relatively robust frame work before the production test.
- (2) When depressurizing, MH's dissociated and the robust MH bearing sand layers (frame work) broke down and caused a decrease in the shear stiffness. Methane gas, dissociated water, and sand grains were released and discharged into the well bore.
- (3) After the production test (when the pump was stopped), MH and sand grains were replaced by formation water or borehole fluid (suggested from the increase in RST sigma, and APSC). P-wave was not excited after the test because of residual gas (suggested from shear slowness of Sonic Scanner).

On the other hand, it is difficult to assume that there are large cavities between the cement and formation considering that S-wave was transmitted to the formation and detected by the Sonic Scanner. Therefore, all we could suggest at present stage might be selective porosity increase by hydrate dissociation and sanding, and residual gas existence.

CONCLUSIONS

We obtained valuable new data about MH bearing formations and hydrate occurrence from open hole wire-line logging. Based on the logging data and production numerical simulation results, we determined the production (zone A) and water injection intervals of 2L-38 (2007) as below.

- (a) Production interval: 1093-1105 mKB
(Total 12m, continuous)
- (b) Water injection interval: 1224-1230, 1238-1256 and 1270-1274 mKB

Three cased-hole logging services, RST, APS and Sonic Scanner were carried out to evaluate physical property changes of the MH bearing formation throughout the production test. At the perforation interval of the MH bearing formation (1093 – 1105 mKB) we noticed a selective dissociation (sand production) in the lateral direction. It was also suggested that neutron porosity was increased and shear stiffness of the formation frame work was decreased, and small amount of gas was remained.

FUTURE WORKS

In the future, the following studies are necessary.

- A. Borehole seismic data (BARS) analysis by Sonic Scanner to investigate and detect MH dissociation front.
- B. Integrated analysis/interpretation of dissociation front using RST, APS and Sonic Scanner data, taking into consideration both sanding volume and the amount of produced gas (mass balance).
- C. Investigation of borehole wall shape change behind casing using other logging data such as Isolation Scanner.
- D. Three dimensional analysis on heterogeneity of MH bearing formation using Rt Scanner and Sonic Scanner.

ACKNOWLEDGEMENTS

The methane hydrate research program has been carried out by the MH21 research consortium consisting of JOGMEC, AIST, and ENAA, with financial support from METI.

We would like to thank METI, JOGMEC, NRCan, and Aurora Research Institute (Aurora) for giving their permission to publish this report. We would also like to thank Schlumberger for the significant effort to acquire precious wire-line logging data under extreme severe conditions and for the strong support with our well log analysis.

REFERENCES

- [1] Yasuda, M., Dallimore, S.R., The task force for production testings; MH21 Research Consortium for Methane Hydrate Resources in Japan, *Summary of the Methane Hydrate Second Mallik Production Test (2007)*, Journal of the Japanese Association for Petroleum Technology Vol. 72, No. 6 (Nov., 2007), p603-607 (Japanese).
- [2] Murray, D., Fujii, T., Dallimore, S.R., *Developments in Geophysical Well Log Acquisition and interpretation in gas hydrate saturated*

Reservoirs, in Proceedings of the VIth International Conference on Gas Hydrates, Vancouver, B.C. July 6-11, 2008.

[3] Numasawa, M., Dallimore, S.R., Yamamoto, K., Yasuda, M., Imasato, Y., Mizuta, T., Kurihara, M., Masuda, Y., Fujii, T., Fujii, K., Wright, J. F., Nixon, F.M, Cho, B., Ikegami, T., Sugiyama, H., *Objectives and Operation Overview of the JOGMEC/NRCan/Aurora Mallik Gas Hydrate Production Test*; in Proceedings of the VIth International Conference on Gas Hydrates, Vancouver, B.C. July 6-11, 2008.

[4] Fujii, K., Cho, B., Ikegami, T., Sugiyama, H., Imasato, Y., Dallimore, S.R. and Yasuda, M., *Development of a monitoring system for the JOGMEC/NRCan/Aurora Mallik Gas Hydrate Production Test Program*; in Proceedings of the VIth International Conference on Gas Hydrates, Vancouver, B.C. July 6-11, 2008.

[5] Dallimore S.R., Wright J. F., Nixon F. M., Kurihara, M., Yamamoto K., Fujii T., Numasawa M., Yasuda M., Imasato Y. 2008. *Geologic and porous media factors affecting the 2007 Production response characteristics of the JOGMEC/NRCan/Aurora gas hydrate production research well*; in Proceedings of the VIth International Conference on Gas Hydrates, Vancouver, B.C. July 6-11, 2008.

[6] Kurihara, M., Masuda, Y., Funatsu, K., Ouchi, H., Yasuda, M., Yamamoto, K., Numasawa, M., Fujii, T., Narita, H., Dallimore, S.R. and Wright, J.F., *Analysis of the JOGMEC/NRCan/Aurora Mallik Gas Hydrate Production Test through Numerical Simulation*; in Proceedings of the VIth International Conference on Gas Hydrates, Vancouver, B.C. July 6-11, 2008.

[7] Dallimore, S.R., Uchida, T. and Collett, T.S. 1999. *Scientific results from JAPEX/JNOC/GSC Mallik 2L-38 gas hydrate research well, Mackenzie Delta, Northwest Territories, Canada*, Geological Survey of Canada, Bulletin 544, 403p.

[8] Collett, T.S., R.E. Lewis, S.R. Dallimore, M.W. Lee, T.H. Mroz, and T. Uchida, *Detailed evaluation of gas hydrate reservoir properties using JAPEX/JNOC/GSC Mallik 2L-38 gas hydrate research well downhole well-log displays*, GSC Bulletin 544, p295-311, 1999.

[9] Collett, T.S., Lewis, R.E., and Dallimore S.R., *JAPEX/JNOC/GSC et al. Mallik 5L-38 gas hydrate production research well downhole well-log and core montages*, GSC Bulletin 585, 2005.

[10] Schlumberger, *Wireline Services Catalog 2007*.

[11] Freedman, R., Minh, C.C., Gubelin, G., Freeman, J.J., McGuinness, T., Terry, B. and Rawlence, D. , *Combining NMR and Density Logs for Petrophysical Analysis in Gas-Bearing Formations*, Paper II, presented at 39th SPWLA Symposium, 1998.

[12] Akihisa, K., Tezuka, K., Senoh, O. and Uchida, T., 2002, *Well log evaluation of gas hydrate saturation in the MITI-Nankai-Trough well, offshore south-east Japan*, SPWLA 43rd Annual Logging Symposium, Oiso, Japan, Paper BB.s

[13] Kenyon, W.E., 1992. *Nuclear magnetic resonance as a petrophysical measurement*, Nuclear Geophysics, 6 (2): 153-171.

[14] Stambaugh, B.J., *NMR tools afford new logging choices*, Oil & Gas Journal; Apr 17, 2000; 98, 16; Platinum Periodicals p 45-52.

[15] Kleinberg, R.L., Flaum, C., Griffin, D.D., Brewer, P.G., Malby, G.E., Peltzer, E.T., and Yesinowski, J.P., 2003, *Deep sea NMR: Methane hydrate growth habit in porous media and its relationship to hydraulic permeability, deposit accumulation, and submarine slope stability*: Journal of Geophysical Research, Vol. 108, No. B10, 2508.

[16] Herron, M.M., Herron, S.L., Grau, J.A., Seleznev, N.V., Phillips, J., Sherif, A.E, Farag, S., Horkowitz, J.P., Neville, T.J., Hsu, K., *Real-Time Petrophysical Analysis in Siliciclastics From the Integration of Spectroscopy and Triple-Combo Logging*, SPE Annual Technical Conference and Exhibition, San Antonio, Texas, 2002(SPE 77631).

[17] Kurihara, M., Ouchi, H., Inoue, T., Yonezawa, T., Masuda, Y., Dallimore, S.R., and Collett, T.S., *Analysis of the JAPEX/JNOC/GSC et al. Mallik 5L-38 gas hydrate thermal-production test through numerical simulation*, In: S.R. Dallimore & T.S. Collett (Eds), *Scientific Results from the Mallik 2002 Gas Hydrate Research Well Program*, Mackenzie Delta, Northwest Territories, Canada., Geological Survey of Canada, Bulletin 585, 2005.

[18] Masuda, Y., Konno, Y., Iwama, H., Kawamura, T., Kurihara, M., Ouchi, H., *Improvement of Near Wellbore Permeability by Methanol Stimulation in a Methane Hydrate Production Well*, Proceedings of 2008 Offshore Technology Conference, Houston, Texas, U.S.A., 2008 (OTC 19433).

[19] Schlumberger, *Introduction to cased hole logging (C.5), RST Reservoir Saturation Tool*.

[20] Inamori, T., Fujii, T., Takayama, T., Saeki, T., Yamamoto, K., *A trial of monitoring of the methane hydrate-production test by sonic well*

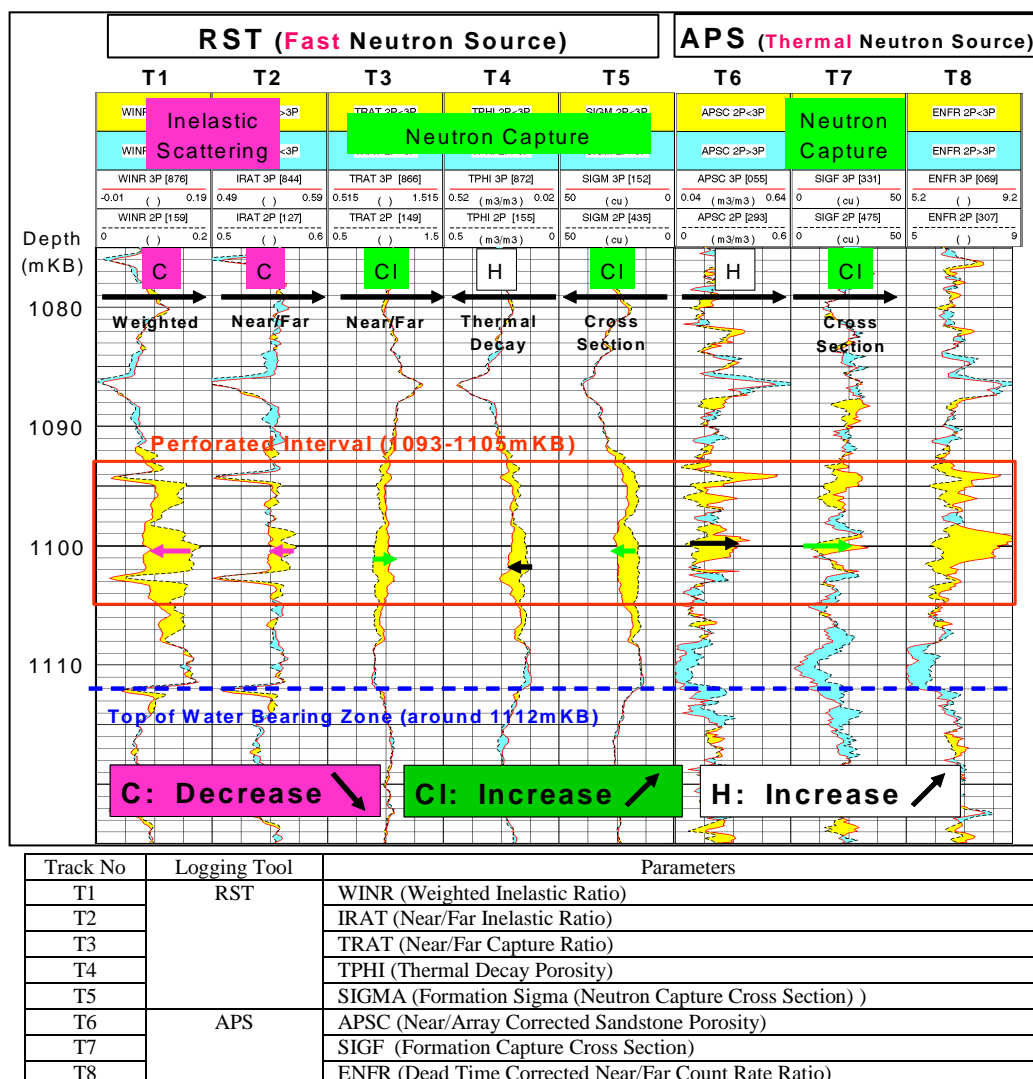


Figure 6. RST and APS change throughout the production test (Zone A).

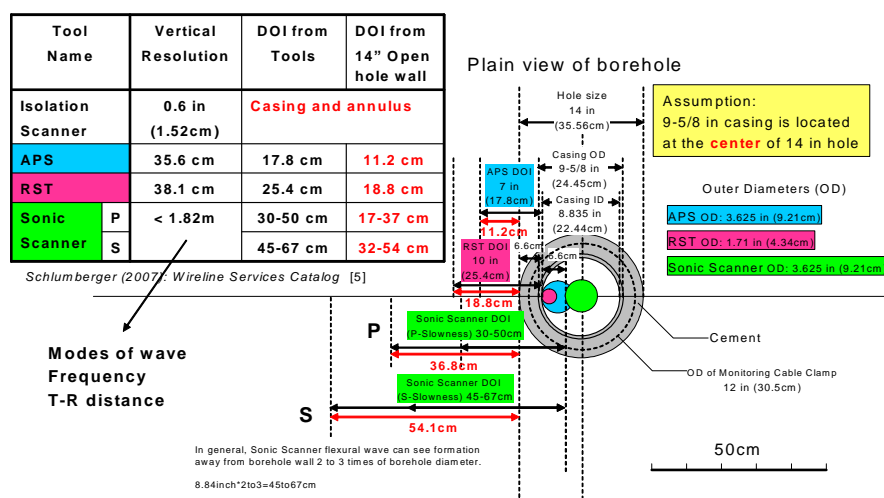


Figure 7. Vertical resolutions and depth of investigations (DOI) of applied cased hole logging tools.

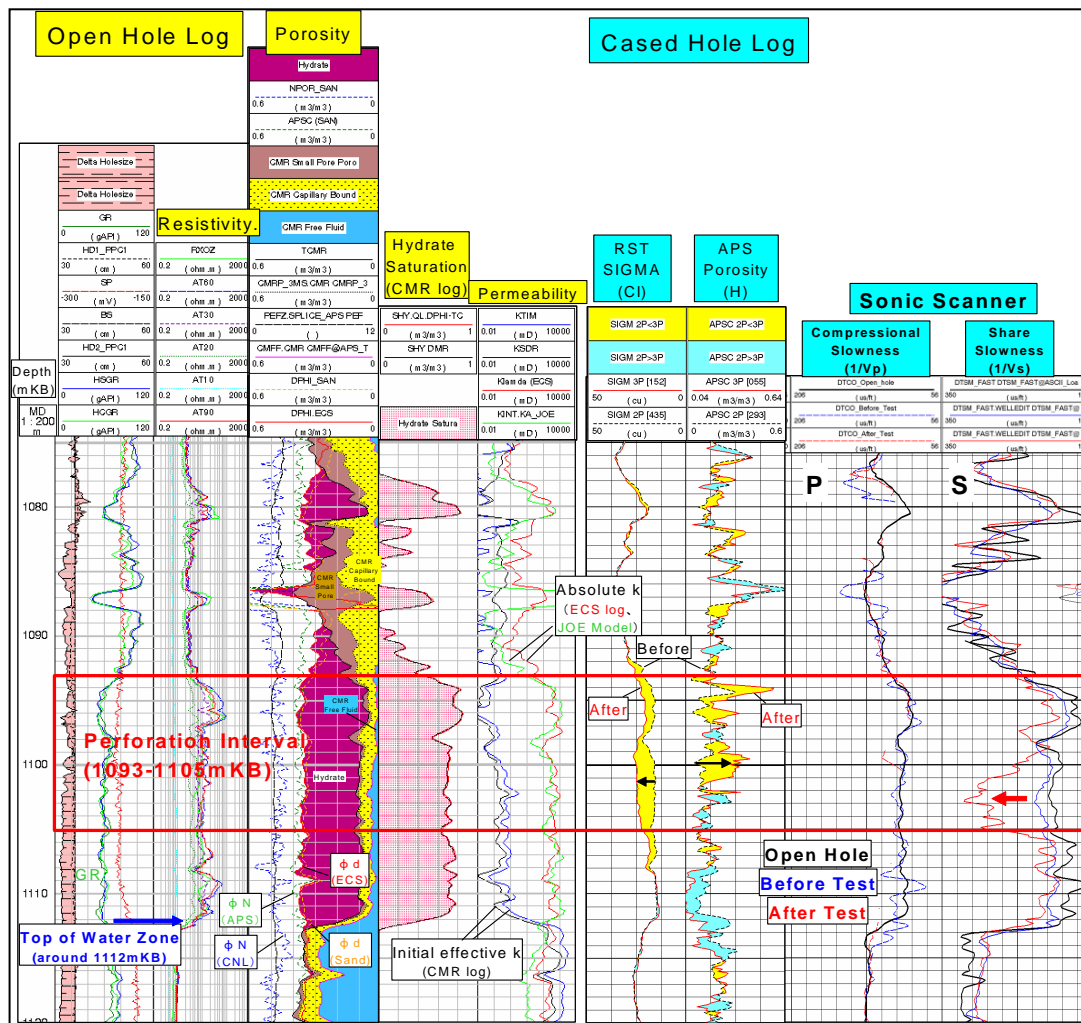


Figure 8. MH bearing formation properties from open hole logs, and the change in cased hole logging response throughout the production test in Zone A, Mallik 2L-38 (2007)

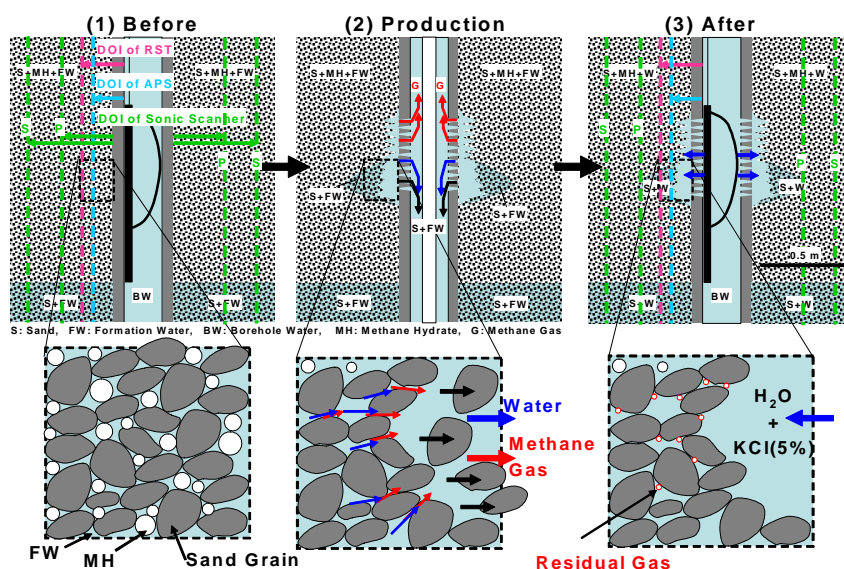


Figure 9. Possible interpretation of MH bearing formation property changes based on RST, APS, Sonic Scanner, and sanding information.